Biol. Cybern. 62, 381–391 (1990)

Biological Cybernetics

Cat and Monkey Cortical Columnar Patterns Modeled by Bandpass-Filtered 2D White Noise*

A. S. Rojer[1,2] and E. L. Schwartz[1,2]

[1] Computational Neuroscience Laboratory, Department of Psychiatry, New York University Medical Center, 550 First Avenue, New York, NY 10016, USA
[2] Department of Computer Science, Courant Institute of Mathematical Sciences, New York University, 251 Mercer Street, New York, NY 10012, USA

Abstract. A simple algorithm based on bandpass-filtering of white noise images provides good quality computer reconstruction of the cat and monkey ocular dominance and orientation column patterns. A small number of parameters control the frequency, orientation, "branchedness", and "regularity" of the column patterns. An oriented (anisotropic) bandpass filter followed by a threshold operation models the macaque ocular dominance column pattern and cat orientation column system. An unoriented (isotropic) bandpass filter models the cat ocular dominance column pattern and the macaque orientation column system. The resemblance of computer graphic simulations produced by this algorithm and histological pattern data, is strong. Since this algorithm is very fast, we have been able to extensively explore its parameter space in order to determine filter parameters which closely match the structure of the various cortical systems. In particular, we have applied spectral analysis to our recent computer reconstruction of the macaque ocular dominance column system, and the model produced by the present algorithm is in close agreement with this detailed data analysis.

1 Introduction

Since the classic electrophysiological observations of Hubel and Wiesel (Hubel and Wiesel 1962) and Mountcastle (Mountcastle 1957), it has been known that cortical neurons with common response properties tend to be grouped together in macroscopic patterns within a cortical lamina. The large scale patterns of neurons which share some common anatomical or functional feature are referred to generically as "columns".

The first direct anatomical reconstruction of the macaque ocular dominance column (ODC) system was provided by (LeVay et al. 1975), based on the use of silver staining. More recent anatomical techniques, such as cytochrome oxidase and 2-deoxyglucose, have also provided views of this and other cortical column systems. In previous work (Schwartz et al. 1988), we demonstrated the application of computer-aided anatomy to permit accurate reconstruction, from serial sections, of the macaque ocular dominance column pattern as revealed by cytochrome oxidase staining (Fig. 1). The availability of accurate computer reconstruction of 2D and 3D patterns of cortical columnar (and topographic) patterns motivated us to develop a parametric algorithm for modeling these phenomena.

At a macroscopic level, cortical column systems can often be described as "stripes" or "blobs" of neurons with common stimulus preferences (e.g. orientation or ocularity). The natural question that is raised is one of efficient description: what is the most economical means of quantitatively describing (and synthesizing) such patterns. The "stripe-like" nature of the ODC system suggests a frequency domain description. The irregularity, branching, and non-uniformity of this and other column systems suggests that a stochastic component is appropriate. The binary (right/left) nature of ODC data is suggestive of a threshold function.

It is common practice in computer graphic modeling of wave-like natural phenomena, such as the texture of marble (Perlin 1985), wind-driven ocean waves (Mastin et al. 1987) and other quasi-periodic phenomena, to use bandpass-filtered noise to create the desired pattern. This observation, along with the above considerations on the nature of the column pattern, led us to explore the use of bandpass-filtered

* This work was supported by AFOSR 88-0275, the Nathan Kline Psychiatric Institute and the System Development Foundation

Fig. 1. Pattern of ocular dominance in macaque determined by computer reconstruction of the brain from serial sections (Schwartz et al. 1988)

noise as a basis for the synthesis of cortical column patterns.

The goal of the present study is to provide a simple description of the cortical column patterns (especially macaque ODC) which is constructive (i.e. is associated with an algorithm), which has as few parameters as possible, and which is capable of providing a suitable synthesis of the pattern which captures the visually evident "branching", "parallelism", etc. of the column patterns. We found that simple parametric models, based on bandpass-filtered noise followed by thresholding or gradient extraction and binning into "columnar" regions, are capable of providing a convincing representation of the structure of the cat and primate ODC and orientation column systems.

In this paper, the properties of bandpass-filtered noise will be demonstrated using isotropic (unoriented) and anisotropic (oriented) filters. We will present algorithms for the modeling of orientation preference and ocular dominance patterns in striate cortex in both cat and monkey, and will conclude with some discussion of the relationship between our pattern-level modeling and more conventional cellular models of columnar structure.

2 One-Dimensional Bandpass-Filtered Noise

It is instructive to examine bandpass-filtered noise in one dimension. We form a one-dimensional white noise signal $f(x)$, by assigning signal values independently for each x according a Gaussian distribution, as shown in Fig. 2a. The kernel of a bandpass filter $h(x')$ is shown in Fig. 2b. For simplicity, we use a band-pass kernel which is a product of a Gaussian with a cosine. In the frequency domain, the filter has the functional form of a pair of symmetrically placed Gaussian passbands

$$H(s)=\exp\left(-\pi\frac{(s-s_0)^2}{\sigma^2}\right). \tag{1}$$

In the frequency domain, the parameter s_0 determines the center frequency of the bandpass and the parameter σ determines the width of the passband. In the space domain, σ determines the number of "lobes" in the kernel, while s_0 determines the spacing of the lobes. As σ decreases, the number of lobes increases, and the kernel approaches a pure sinusoidal waveform with frequency determines by s_0: its passband approaches zero. The result of convolution of the kernel with the noise signal

$$g(x)=h(x)*f(x)=\int_{-\infty}^{\infty} h(x-x')f(x')\mathrm{d}x' \tag{2}$$

is shown in Fig. 2c. The creation of an irregular yet mainly periodic signal is evident. Finally, in Fig. 2d, we show the results of thresholding the filtered noise signal according to

$$G(x)=\begin{cases}0, & \text{if } g(x)<0;\\ 1, & \text{otherwise}.\end{cases} \tag{3}$$

The one-dimensional "columns" have the approximate form of a square wave; a smoother, but qualitatively similar pattern would be obtained with a sigmoidal pixel transfer function (which we will consider below).

3 Isotropic Two-Dimensional Bandpass-Filtered Noise

The defining property of a noise image is that the values of neighboring pixels are independent and drawn from identical Gaussian probability distributions. The noise image is characterized by the mean μ and standard deviation σ of the underlying Gaussian distribution.

For a two-dimensional signal (e.g. an image), the frequency variable s is two-dimensional. These two dimensions may be interpreted as describing the orientation and (scalar) frequency[1] of a planar sinusoid

[1] In this paper, we use frequency units such that unity corresponds to the highest frequency represented. This allows us to freely compare systems with different physical scales

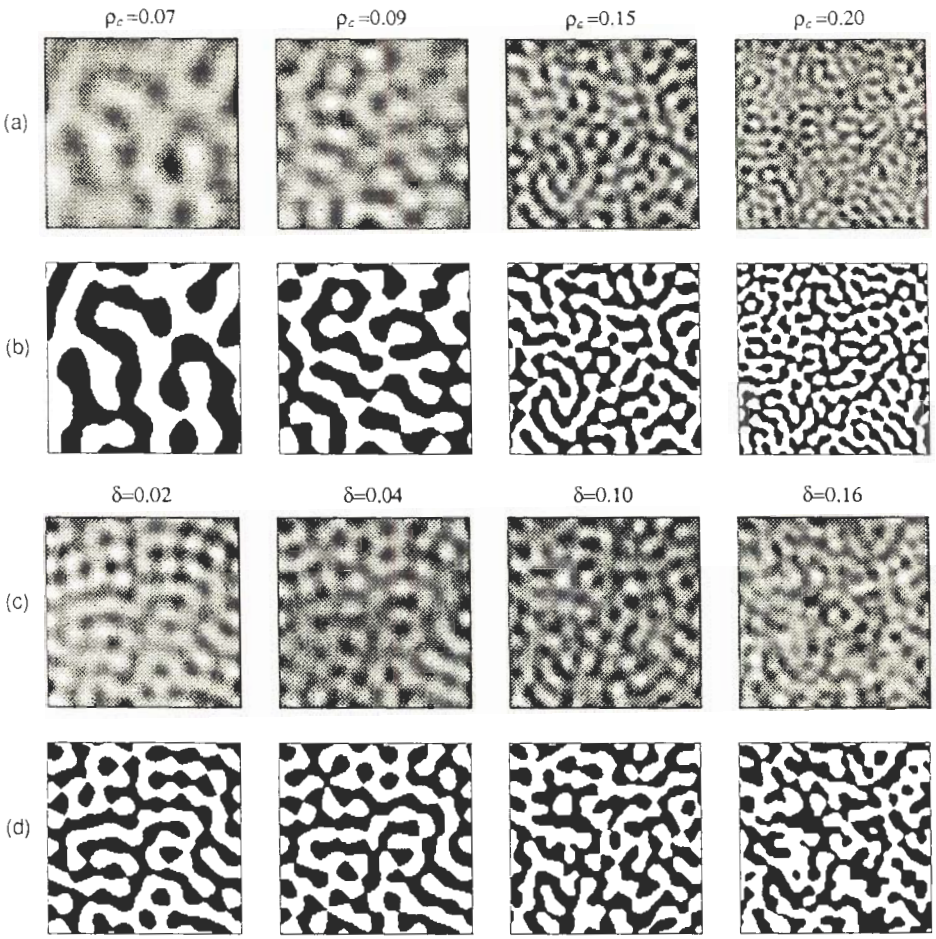

Fig. 4a–d. Parametric characteristics of thresholded isotropic (unoriented) bandpass-filtered noise. **a** Variation of the center frequency $\varrho_c = \frac{1}{2}(s_1 + s_2)$, constant bandwidth $\delta = 0.06$. **b** Midrange threshold of **a**. **c** Variation of the bandwidth $\delta = s_1 - s_2$, constant center frequency $\varrho_c = 0.12$. **d** Midrange threshold of **c**

pass filters according to the frequency domain structure:

$$H(s) = \sigma(s_1 - s)\sigma(s - s_2), \tag{4}$$

with $\sigma(x)$ a sigmoidal function

$$\sigma(x) = \frac{1}{1 + \exp(-\alpha x)}. \tag{5}$$

Thus, the isotropic bandpass filter is characterized by three parameters, a low-pass cutoff s_1, a high-pass cutoff s_2 and a rise-time determined by α. Equivalently, we may refer to the center frequency $\varrho_c = \frac{1}{2}(s_2 + s_1)$ and the bandwidth $\delta = s_2 - s_1$, which correspond respectively to the center radius and width of the annulus in the frequency domain. An example of a filtered noise image is shown in Fig. 3c.

The effects of parameter modification for the isotropic bandpass are shown in Fig. 4. Increasing the scalar frequency parameter ϱ has the effect of scaling the image (a sort of reverse zoom). Increasing the bandwidth parameter has the effect of diminishing the regularity of the column width.

4 Two-Dimensional Anisotropic Bandpass-Filtered Noise

The kernel of an oriented (anisotropic) filter is described by "humps" centered on symmetric points in the frequency domain (Fig. 5a). The center point of the humps corresponds to a planar sinusoid of particular scalar frequency and orientation. The space-domain kernel of the filter consists of alternating positive and negative regions in the direction perpendicular to the preferred orientation, with the regions elongated parallel to the preferred orientation (Fig. 5b). Filtered noise assumes a wave-like pattern (Fig. 5c).

The anisotropic bandpass filter requires more parameters than the isotropic filter: formally we implement it in the frequency domain with a symmetric pair of binormal Gaussian blurs centered on s_0, with

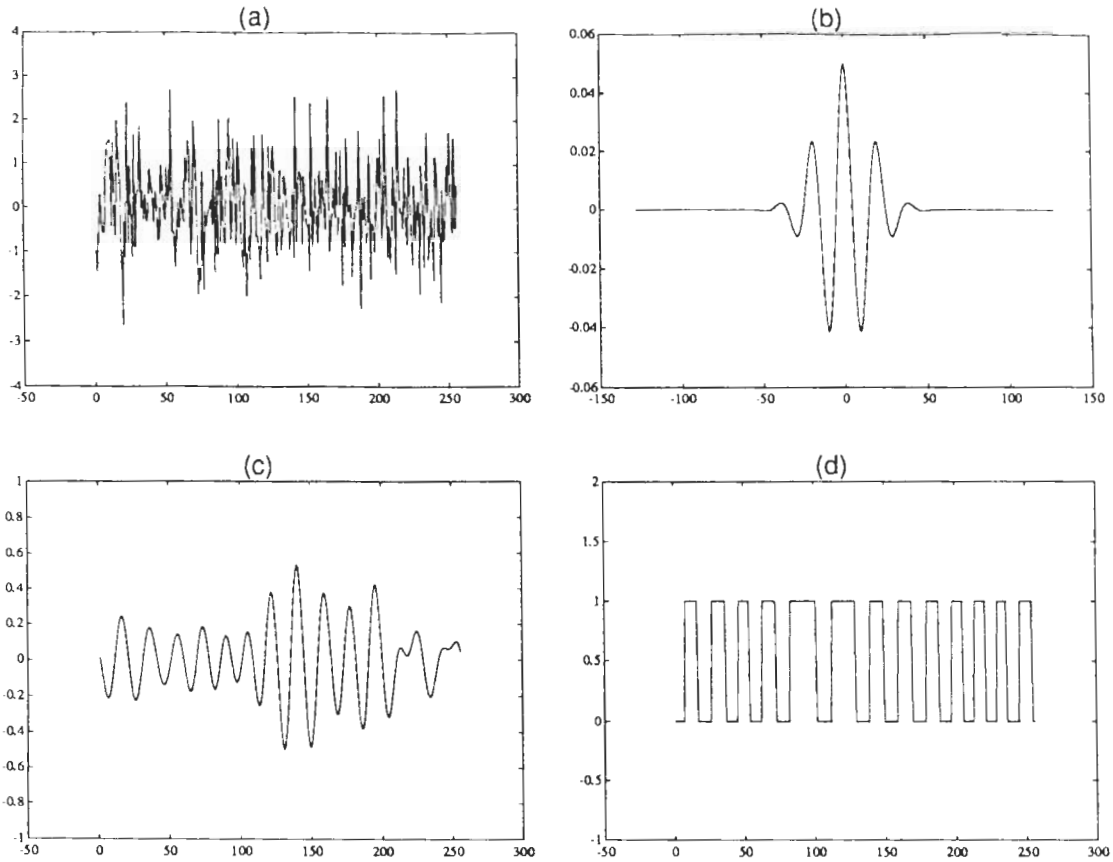

Fig. 2a–d. One dimensional demonstration of the qualitative characteristics of bandpass-filtered noise. **a** Zero mean, unit standard deviation Gaussian noise. **b** The (space domain) kernel of a typical bandpass filter. **c** The convolution of the kernel in **b** with the noise signal in **a**. **d** The "columns" which result when the signal in **c** is thresholded

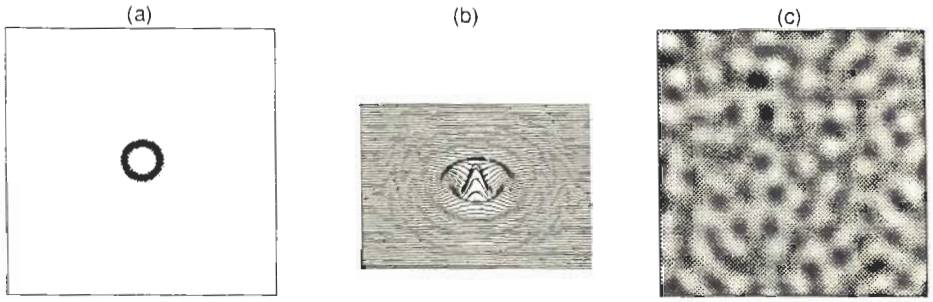

Fig. 3a–c. Two dimensional demonstration of the qualitative characteristics of unoriented (isotropic) bandpass-filtered noise, shown as intensity plots. **a** A typical isotropic bandpass filter in the frequency domain. **b** The (space domain) kernel of the filter shown in **a**. **c** The convolution of the kernel in **b** with white noise

(Bracewell 1978). Formally, if $s=(u, v)$, we can define $\varrho=(u^2+v^2)^{1/2}$ as the scalar frequency or frequency magnitude, and $\theta=\tan^{-1}(v/u)$ as the orientation. The inverse Fourier transform of a nonzero value at s is the planar sinusoid with $1/\varrho$ pixels between wave crests, and with normals to the wave crests pointing in direction θ. For a fixed θ, as ϱ increases the wave crests move closer together. Similarly, as θ increases by $\delta\theta$, the "grating" is rotated by $\delta\theta$.

The decomposition of two-dimensional frequency signals into orientation and scalar frequency permits a characterization of two-dimensional bandpass filters according to orientation preference. When a filter has no preferred orientation, we say it is isotropic. In this case, the filter has an annular shape in the frequency domain (Fig. 3a); in the space domain we find a kernel which has a familiar center-surround structure (Fig. 3b). Formally, we will represent isotropic band-

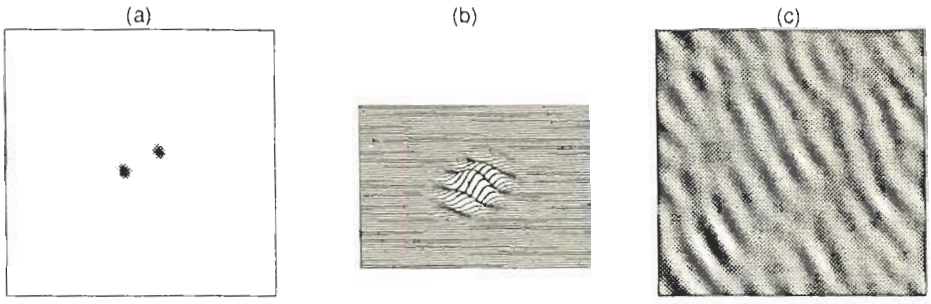

Fig. 5a–c. Two dimensional demonstration of the qualitative characteristics of oriented (anisotropic) bandpass-filtered noise. **a** The frequency domain representation of an anisotropic bandpass filter. **b** The (space domain) kernel of the filter shown in **a**. **c** The convolution of the kernel in **b** with a white noise image

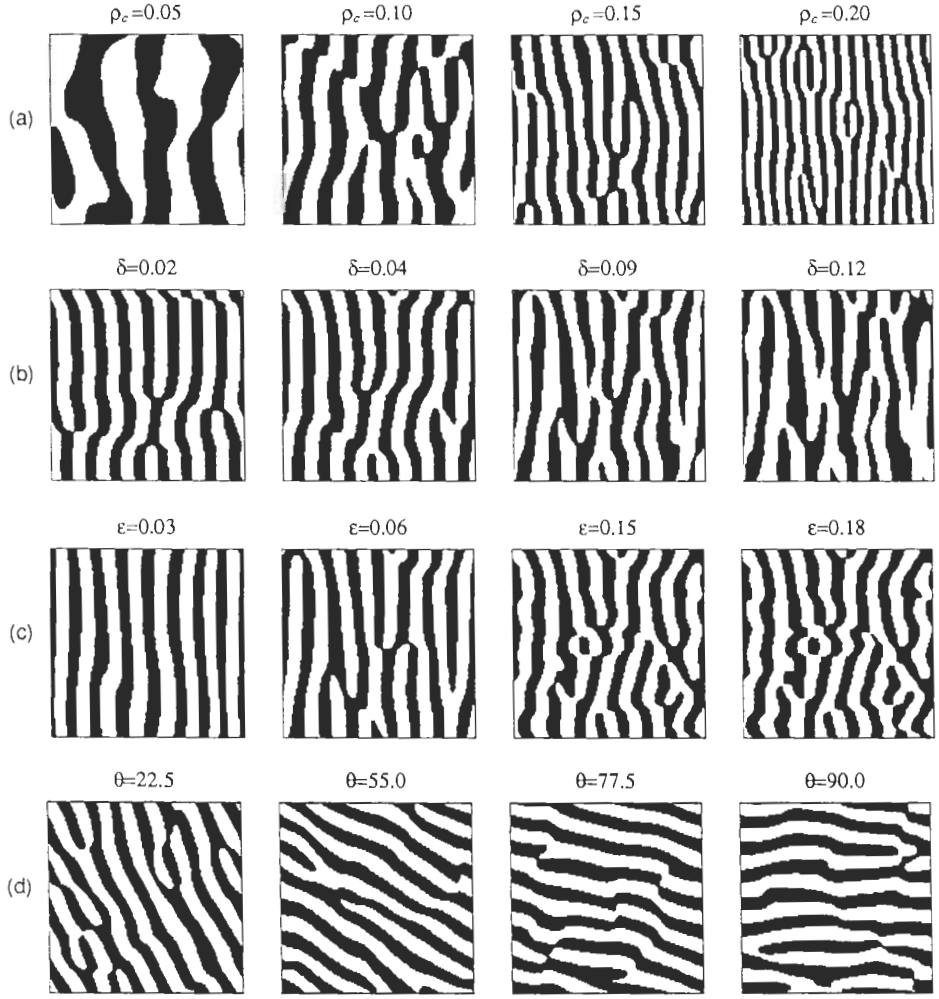

Fig. 6a–d. Parametric characteristics of thresholded anisotropic (oriented) bandpass-filtered noise. **a** Variation of the center frequency $\varrho_c = \frac{1}{2}(s_1 + s_2)$, constant bandwidth $\delta = 0.06$, constant $\varepsilon = 0.09$, constant $\theta = 0$. **b** Variation of the bandwidth δ (in the direction of the dominant frequency), constant center frequency $\varrho_c = 0.12$, constant $\varepsilon = 0.09$. **c** Variation of the eccentricity ε (perpendicular to the direction of the dominant frequency). Constant bandwidth $\delta = 0.06$, constant center frequency $\varrho_c = 0.12$. **d** Variation of the orientation θ. Constant bandwidth $\delta = 0.06$, constant center frequency $\varrho_c = 0.12$, constant eccentricity $\varepsilon = 0.09$

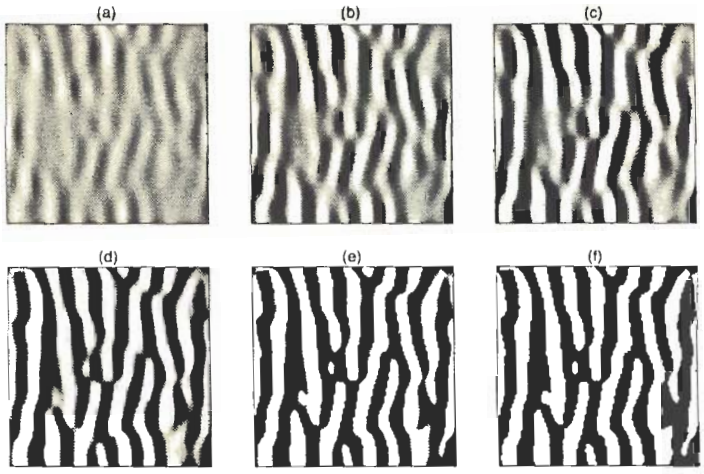

Fig. 7a–f. Effect of sigmoid with on columnar pattern. **a** Bandpass-filtered noise before sigmoid. **b** Sigmoid width 75% of full range. **c** Sigmoid width 50% of full range. **d** Sigmoid width 25% of full range. **e** Sigmoid width 6.25% of full range. **f** Threshold

principal axes oriented normal and parallel to θ_0. This bandpass filter is directly analogous to the one-dimensional bandpass; in the space domain, its kernel is formed by the product of a planar sinusoid with a two-dimensional Gaussian. Four parameters are required for a complete description. Like the isotropic filter, the scalar frequency ϱ_c must be specified. In addition, we need to specify the orientation of the center frequency θ, the width δ parallel to the preferred orientation, and the width ε normal to the preferred orientation.

The effects of variation of these parameters are shown in Fig. 6. Here, we systematically vary the filter parameters and the examine the properties of thresholded, bandpass-filtered white noise. Like the isotropic filter, the scalar frequency ϱ_c provides a scale, determining the column width (Fig. 6, top row). The bandwidth in the direction parallel to the filter orientation δ determines the variation in column width, which we denote "regularity"; at low values, the column width is uniform (Fig. 6, second row). The bandwidth normal to the filter orientation ε determines the "branchiness" of the columns (Fig. 6, third row). At high values, the columns are prone to sudden shifts of orientation, and column boundaries are irregular. Changing the orientation parameter has the effect of rotating the stripes (Fig. 6, lower row).

One physiological parameter observed in single-cell studies is the degree of ocular preference as one traverses a pair of columns. We model ocular dominance at a point in the cortex to be a continuous variable ranging over [0, 1]. At any given location, the magnitude of the variable corresponds to the degree of preference for an particular eye, with 0 complete absence of preference and 1 complete dominance. In layer IV of area V1 in the macaque (LeVay et al. 1975), an abrupt transition occurs from total dominance by one eye to total dominance by the other eye (e.g. from 0 to 1 in a short distance). The cat ODC system (Hubel and Wiesel 1962) seems less "hard-edged" than that of the macaque, with significant numbers of cells showing balanced preferences (i.e. a gradual transition from 0 to 1, with more cells near $\frac{1}{2}$).

The transition of both the cat and monkey columns may be modeled generally by a sigmoid function (5). In the event $\alpha > 0$, as $x \to -\infty$, $\sigma(x) \to 0$. Similarly, as $x \to \infty, \sigma(x) \to 1$. The abruptness (equivalently, width) of the transition is controlled by the parameter α; as α gets large, the transition takes place over a shorter range. In the limit $\alpha \to \infty$, $\sigma(x)$ becomes a threshold function.

We use the sigmoid to generalize from the threshold to cases where ocular dominance is not complete; Fig. 7 shows a progression from an unprocessed anisotropic bandpass-filtered noise image to a threshold via sigmoids of increasing abruptness (decreasing width). In addition to providing a model for degrees of ocular preference, the successively steepening sigmoid applied to bandpass-filtered anisotropic noise may provide a useful pattern-level model for the development of ocular dominance. Experimental results relating to the temporal formation of ODC in the monkey and cat may be found in (Hubel et al. 1977; LeVay et al. 1978).

5 Analysis and Modeling of the Ocular Dominance Column Pattern

The macaque ODC system (Fig. 1) is characterized by elongated stripes of slowly varying orientation, relatively constant local width, and a small degree of branching (LeVay et al. 1975; LeVay et al. 1985; Schwartz et al. 1988). A superficial similarity to the thresholded, anisotropic-filtered noise in Fig. 5 and Fig. 6 is immediately evident. The relatively constant local width is consistent with a bandpass filter centered on the scalar frequency corresponding to the column

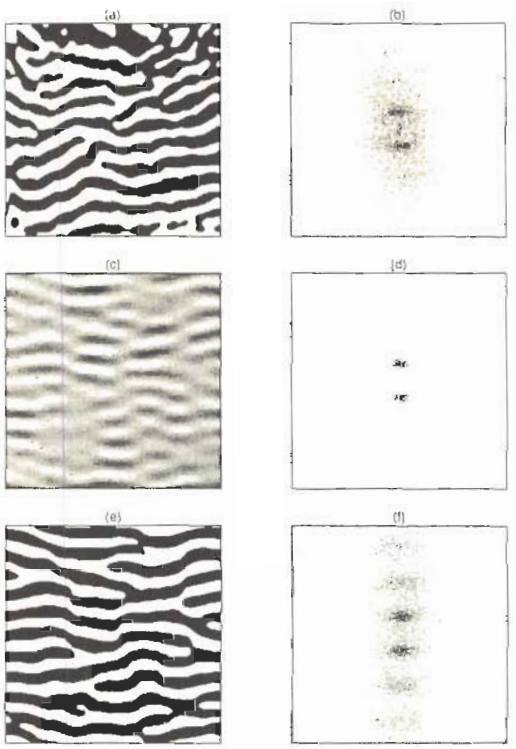

Fig. 8a–f. Examples of subimage analysis from the flattened brain. **a** A section from the flattened ocular dominance pattern. **b** The spectrum of **a**. From this spectrum, we derived filter parameters $f_c = 0.25$, $\theta = 18$ deg, $\delta = 0.15$, and $\varepsilon = 0.20$. **c** An image synthesized by application of the filter parameters derived from **b** to Gaussian noise. **d** The spectrum of the synthetic image (i.e. the convolution of the derived filter with a Gaussian noise). **e** Threshold applied to **c**. **f** The spectrum of **e** compare to **b**

period. The high degree of local parallelism requires an anisotropic filter to restrict the orientation of the bandpass (over small distances). These qualitative observations are borne out by examination of the local power spectra of the macaque ocular dominance pattern. Figure 8a shows a section of the ODC pattern which has been further processed to obtain a clean binary signal; the corresponding spectrum is shown in Fig. 8b.

The position and shape of the peaks in the spectrum of the subimage can be characterized by their centroid and the principal axes about the centroid, which are readily computed. Figure 8c shows the result of application of the filter derived from this fitting procedure to white noise; the corresponding (synthesized) spectrum is shown in Fig. 8d. The synthesized spectrum can be seen to correspond to the measured spectrum with respect to location of peaks and rough shape of the peaks. In Fig. 8e, we have applied a threshold to the synthetic pattern, obtaining a synthetic column pattern which strongly resembles the measured pattern in both the space and frequency domain.

By restricting this analysis to first and second moments of the local power spectra, we assumed a Gaussian shape for the filter kernel (in the frequency plane). However, the actual spectra of the data appear to have more "tail" than a Gaussian distribution. This is reflected in the space domain; the synthetic image has the right amount of "branching", but in the synthetic image, the column regularity is too large. It is likely that these residual details could be improved by using a more sophisticated fitting procedure on the power spectra (e.g. third and higher order moments), but at the cost of additional parameters in the description.

Another significant difference between the actual data and the model is the change in column orientation over the subimage; in the data, orientation appears constant over roughly 3–5 column widths, but for larger scales it is prone to small shifts. In the synthetic image, however, we are restricted to a single orientation. In other work, we will examine the issue of parameter variation over the cortical surface; here we are merely trying to demonstrate the similarity of the synthetic and actual data over short distance scales.

The results of Fig. 4 (thresholded isotropic bandpass-filtered noise) provide a good model of recent data on the cat ocular dominance column system (Anderson et al. 1988)[2]. Figure 10 shows a comparison of this data of (Anderson et al. 1988) and one of the parametric example from Fig. 4.

6 Models for Orientation Columns

The bandpass-filtered noise depicted in Fig. 3c has a strong resemblance to published measurements of the magnitude of the *gradient* of preferred orientation in monkey striate cortex (Blasdel and Salama 1986), as measured by voltage-sensitive optical dyes. The observed pattern of orientation selectivity is characterized by whorl-like circular progressions of selectivity interspersed with trough-like regions of roughly uniform orientation selectivity. Similarly, the bandpass-filtered noise has a structure of circular humps of positive or negative character against a background of irregular, linearly extended columnar regions with little sign preference.

Because orientation columns are characterized by regions of shared directional preference for changes of contrast, we reasoned that the direction of the gradient of image intensity might be useful for column synthesis. A hump-like pattern in the filtered noise yields a whorl-

[2] We thank Prof. Michael Stryker for pointing out the similarity of the data of Anderson et al. (1988) and our simulation

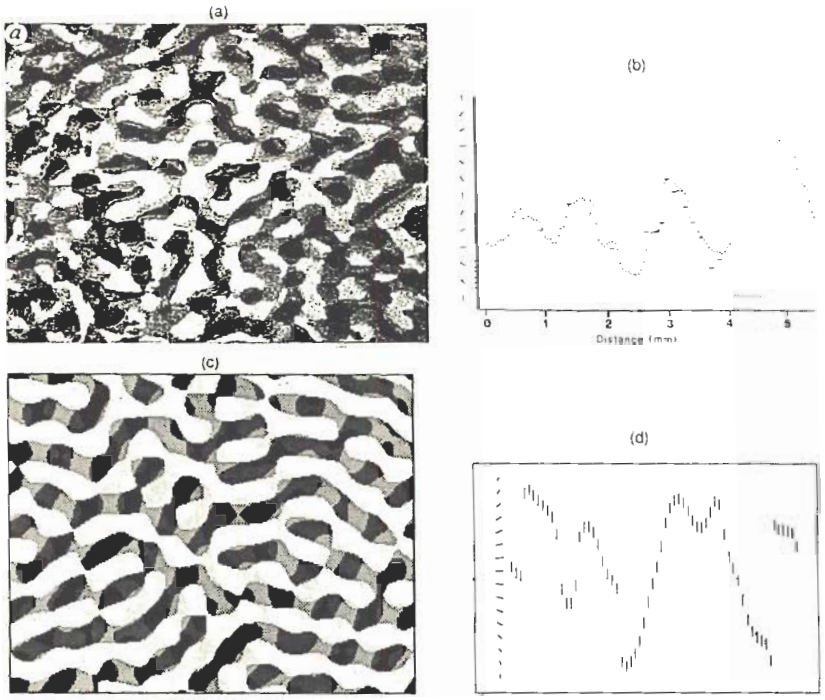

Fig. 9a–d. Orientation columns modeled by isotropic bandpass filtering of noise. Bandwidth $\delta = 0.015$, center frequency $\varrho_c = 0.0775$. **a** Orientation columns determined by voltage sensitive optical dye, grouped into six classes (Blasdel and Salama 1986). **b** A simulated electrode traversal in the data **a** (Blasdel and Salama 1986). **c** Columns formed by extraction of image intensity gradient direction from bandpass-filtered noise. Results are banded into six regions of roughly common directional preference to facilitate comparison with **a**. **d** A simulated electrode traversal in the model image **c**

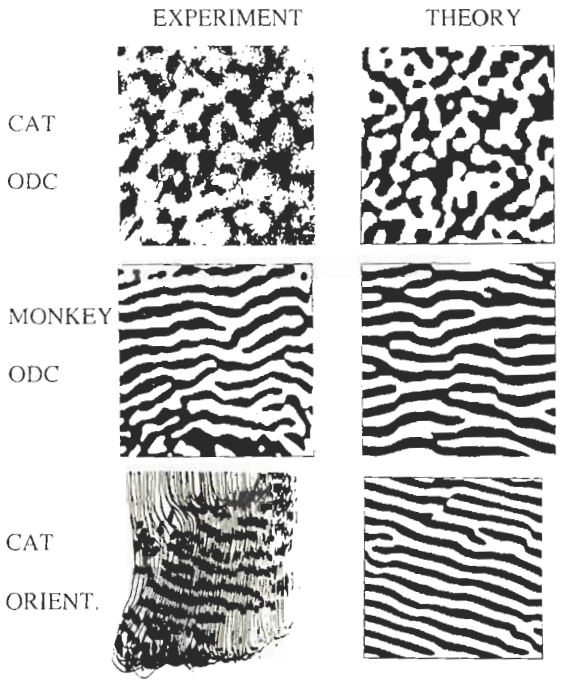

like pattern of gradient direction, and a trough-like pattern in the filtered noise yields a region of uniform gradient direction. These effects may be seen in Fig. 9, which shows the result of computation of the direction of the gradient of image intensity for isotropic bandpass-filtered noise. Figure 9a shows measurements of orientation preference in macaque cortex determined by voltage-sensitive optical dye (Blasdel and Salama 1986). Figure 9b shows the expected measurement of orientation preference determined by an electrode traversing the region of cortex depicted in Fig. 9a. In Fig. 9c, we constructed synthetic orientation columns by extraction of the direction of intensity gradient from an isotropic bandpass-filtered noise image. Regions of similar preference have been grouped to facilitate comparison with Fig. 9a. In Fig. 9d, a simulated electrode traversal through the synthetic columns is shown.

Fig. 10. Comparison of histological data (column labeled "EXPERIMENT") of several cortical columnar systems, with band-pass filtered noise (column labeled "THEORY"). *Top row:* Cat ocular dominance system, area 17. Experimental data reprinted from (Anderson et al. 1988). Data was obtained by transneuronal transport of wheat germ agglutinin horseradish peroxidase, injected into ipsilateral eye. Theoretical data was constructed by isotropic band-pass filtered noise, using center frequency $\varrho_c = 0.12$, band-width $\delta = 0.06$. *Middle row:* Monkey ocular dominance system, area 17 (striate cortex). Experimental data reprinted from (Schwartz et al. 1988). Data was obtained from cytochrome oxidase stain following contralateral eye enucleation (one month), and computer reconstruction and flattening of serial sections. Theoretical data was constructed by anisotropic band-pass filtered noise, using center frequency $\varrho_c = 0.25$, band-width $\delta = 0.15$, and eccentricity $\varepsilon = 0.20$. *Bottom row:* Cat orientation column system, area 18. Experimental data reprinted from (Singer 1981). Data was obtained from 2-deoxyglucose autoradiography, following stimulation with vertical gratings. Theoretical data was constructed from anisotropic band-pass filtered noise, using center frequency $\varrho_c = 0.18$, band-width $\delta = 0.07$, eccentricity $\varepsilon = 0.12$

Figure 10 summarizes the results of our application of thresholded bandpass-filtered noise to model cortical column systems. We show comparison of theory and experiment for monkey and cat ODC, as well as cat orientation columns (Singer 1981) determined by 2DG mapping. Curiously, a two-by-two table of cat and monkey, versus ocular and orientation columns, shows the following pattern: cat ocular and monkey orientation columns are derived with an isotropic mechanism, whereas cat orientation and monkey ocular columns are derived with an anisotropic mechanisms.

7 Discussion

In the context of explicit modeling of the ODC system, it was originally suggested that the column system is the result of a joint "excitatory-inhibitory" or "competitive" interaction (LeVay et al. 1975). Swindale (1980) developed this idea using an isotropic excitatory local interaction in competition with an inhibitory mechanism of slightly larger range. This model produced patterns which were reminiscent of the macaque ODC system, but which lacked the long-range correlation of orientation which is such a striking feature of the data. In order to describe the macaque ODC pattern, Swindale suggested a modification of his model which incorporated "stretching" in one direction, resulting in a closer resemblance to the actual pattern. However, Swindale did not further explore or define the parameter space of anisotropic mechanisms; moreover, the results still did not capture the branching aspect of macaque PDC pattern.

Swindale's model is essentially equivalent to convolution of an isotropic center-surround mechanism with noise, followed by a threshold. The center-surround is provided by "developmental" mechanisms which are facilitatory at short range, but which are competitive at longer range. Local ocular preference in Swindale's model is self-reinforcing, but limited by a fixed upper bound on "synaptic" strength. This leads to a threshold-like dynamic; once a region has a stable preference for one ocularity, it is enhanced by self-reinforcement to the limiting value for ocular preference. This "bounded positive feedback" is in close analogy to an iterated sigmoid; depending on the initial condition (positive or negative), successive iteration of the sigmoid (suitably anti-symmetrized to range over $[-1, 1]$) will have the consequences of a self-reinforcement.

Linsker recently provided a model of the macaque orientation column system (Linsker 1986). This model is complex, has many parameters, and is difficult to briefly summarize. However, it is apparent that an essential characteristic of the system is an isotropic center-surround architecture, combined with something closely resembling iterated convolution. Figure 9 depicts the results of our model for orientation columns in the primate, which is similar to the results obtained by Linsker using a considerably more complicated model.

Miller et al. (1988) have constructed a detailed neural model based on the properties of NMDA receptors, Hebbian interaction, and extensive developmental data on the plasticity of the ODC system in the cat. They model the development of the ODC system as a dynamical system, using stability analysis to determine a dominant frequency (eigenvalue) which predicts the column width in the columnar pattern. They have provided convincing examples of ODC-like patterning in the cat. The filter parameters derived in the present paper which are needed to obtain a good model of the primate ocular dominance column system could perhaps be helpful in extending their neuronal model to primate ocular dominance columns.

Other models of column formation at the cellular level have been proposed. The origin of ODC anisotropy is treated by (Cowan and Malsburg 1985); Orientation column formation is considered by (Swindale 1982) and (Gotz 1987, 1988). These models provide potential sub-columnar mechanisms for the emergence of the bandpass filters which we employ in this work.

The models presented in this paper, which are most easily expressed in terms of frequency domain representations of filters, can be related to space-domain models such as (Linsker 1986; Swindale 1980) via the inverse transform of frequency-domain filter characteristics into space-domain "kernels". In the case of an isotropic filter, the "center" or excitatory aspect of our models is equivalent to a positive spatial correlation of neuronal processes, and the inhibitory "surround" is equivalent to an anti-correlation. A number of mechanisms can provide this local correlation and anti-correlation: chemotaxic interaction, synaptic cooperation/competition, template formation by sub-columnar structures [e.g. cytochrome oxidase blobs; see (Gotz 1988)], correlation of incoming signals with Hebbian adaptation. Our model, of course, does not address the detailed nature of how the bandpass filter (frequency domain) or local correlation-anti-correlation (space domain) is supplied. Rather, we summarize the consequences of this mechanism (or mechanisms!) upon the final observable values of the column pattern itself.

An analogy that characterizes the difference of the present model with those mentioned above is that of fluid mechanics: it is possible to describe fluid motions in terms of large scale patterns (vorticity, streamlines) which ignore the fundamental molecular nature of the

fluid. Complementary to this continuum, descriptive approach is a molecular approach which seeks to describe the large scale patterns of fluid motions from detailed mechanical principles. The continuum approach characterized the early stages of the field, and provided considerable insight into the nature of fluid motion patterns, while the molecular approach provides a more complete description, but at the cost of herculean computational and mathematical effort. Full scale microscopic approaches to fluid dynamics, to the present day, still provide major unsolved numerical and computational frontiers.

In the case of patterns of columnar and topographic structure in primate brain, there seems to be a direct analogy. By focusing on the large scale, or continuum aspect of cortical column, we have found that a simple frequency domain model provides a constructive algorithm for synthesizing the observed neuronal patterns. A small number of parameters in this method can be adjusted to provide highly accurate reproduction of existing data. Moreover, the efficient computational aspects of this model allow us to synthesize full two-dimensional models of various cortical patterns without requiring large scale computational resources. Thus, from a practical viewpoint, we believe that the results of this work provide a significant advantage for simulation studies of visual cortex.

Each of the models reviewed above is capable of accounting (at least qualitatively) for an observed ODC or orientation column pattern. But what is the essential reason for their success? We propose that the basic reason which underlies the ability of these apparently diverse models to model various columnar column patterns is due to the fact the columnar patterns themselves are accurately represented as bandpass-filtered noise followed by a selection operation (e.g. thresholding, gradient extraction, etc.). In the present paper, we have shown that the same algorithm, by adjustment of parameters, can synthesize the cat and monkey ocular dominance and orientation column patterns. We expect that other similar columnar systems (e.g. MT direction columns, V2 thick/thin/interblob) may also be described by a similar formalism.

The simplicity and realizability of this process suggest that a column pattern is a highly likely consequence for any mixing of two or more different systems. Any dynamics which provides the equivalent of a bandpass filter, and a selection operation, is sufficient to qualitatively synthesize these patterns.

8 Conclusion

Our approach to describing and synthesizing columnar patterns in macaque cortex is closely related to current methods in computer graphics used for synthesizing other natural phenomena, such as wind driven ocean waves (Mastin et al. 1987), and marble textures (Perlin 1985). However, it is quite different, both in method and motivation, from other recent models of ocular dominance columns and orientation columns in macaque cortex (Linsker 1986; Malsburg 1979; Miller et al. 1988; Swindale 1980). The latter models begin from the neuronal level of scale, and seek to achieve a final pattern which resembles the anatomical data. We work at the level of the anatomical pattern, without explicit consideration of neuronal processes.

A variety of diverse models have been proposed to explain the development of columnar structure, all of which produce patterns which are more or less similar to that of the observed ocular dominance and orientation column patterns of V1. But there is a relative dearth of experimental data on the details of the developmental and adaptive processes which might be operative at the neuronal level. Previous models have explored a variety of developmental and adaptive mechanisms; perhaps the actual mechanism at work is one which has been considered, one not yet thought of, or some combination of mechanisms. For our purposes, and given an absence of detailed mechanistic information, it is efficient to separate the problem of pattern description from the problem of characterizing the mechanism of pattern formation.

The algorithms of this paper provide what are arguably the simplest means of effectively synthesizing two dimensional columnar pattern which are in close agreement to anatomical data. There may also be some theoretical insight to be gained from this work: the spatial kernels we have utilized to construct synthetic column images may constrain hypotheses of cellular interaction in mechanistic, developmental models.

References

Anderson PA, Olavarria J, Sluyters RCV (1988) The overall pattern of ocular dominance bands in cat visual cortex. J Neurosci 8:2183–2200

Blasdel G, Salama G (1986) Voltage sensitive dyes reveal a modular organisation in monkey striate cortex. Nature 321:579–585

Bracewell RN (1978) The Fourier transform and its applications. McGraw-Hill, New York

Cowan JD, Malsburg C (1985) A proposed mechanism for the origin and development of iso-orientation columns. In: Rose D, Dobson VG (eds) Models of the visual cortex. Wiley, New York, pp 462–472

Gotz KG (1987) Do "*d*-blob" and "*l*-blob" hypercolumns tessellate the monkey visual cortex. Biol Cybern 56:107–109

Gotz KG (1988) Cortical templates for the self-organization of orientation-specific *d*- and *l*-hypercolumns in monkey and cats. Biol Cybern 58:213–223

Hubel DH, Wiesel TN (1962) Receptive fields, binocular interaction, and functional architecture in cat visual cortex. J Physiol 160:106–154

Hubel DH, Wiesel TN, LeVay S (1977) Plasticity of ocular dominance columns in monkey striate cortex. Phil Trans R Soc Lond B 278:131–163

LeVay S, Hubel DH, Wiesel TN (1975) The pattern of ocular-dominance columns in macaque visual cortex revealed by a reduced silver stain. J Comp Neurol 159:559–576

LeVay S, Stryker MP, Shatz CJ (1978) Ocular dominance columns and their development in layer IV of the cat's visual cortex: a quantitative study. J Comp Neurol 179:223–244

LeVay S, Connolly M, Houde J, Van Essen DC (1985) The complete pattern of ocular dominance stripes in the striate cortex and visual field of the macaque monkey. J Neurosci 5:486–501

Linsker R (1986) From basic network principles to neural architecture. Proc Natl Acad Sci 83:8779–8783

Malsburg C (1979) Development of ocularity domains and growth behavior of axon terminals. Biol Cybern 32:49–62

Mastin GA, Watterberg PA, Mareda JF (1987) Fourier synthesis of ocean waves. IEEE Computer Graph Appl March: 16–23

Miller K, Stryker M, Keller J (1988) Network model of ocular dominance column formation: analytical results. Neural Netw 1 [Suppl 1] 266

Mountcastle VB (1957) Modality and topographic organization of single neurons of cat's somatic sensory cortex. J Neurophysiol 20:408–434

Perlin K (1985) An image synthesizer. Comput Graph 19:287–296

Schwartz EL, Merker B, Wolfson E, Shaw A (1988) Computational neuroscience: applications of computer graphics and image processing to two and three dimensional modeling of the functional architecture of visual cortex. IEEE Comput Graph Appl July: 13–28

Singer W (1981) Topographic organization of orientation columns in the cat visual cortex. Exp Brain Res 44:431–436

Swindale NV (1980) A model for the formation of ocular dominance column stripes. Proc R Soc Lond B 208:243–264

Swindale NV (1982) A model for the formation of orientation columns. Proc R Soc Lond B 215:211–230

Received: June 28, 1989
Accepted in revised form: November 10, 1989

Prof. Eric L. Schwartz
New York University Medical Center
Department of Psychiatry
Computational Neuroscience Laboratory
550 First Avenue
New York, NY 10016
USA